Transient Vortex Flow Characteristics in Three-Strand Bloom Tundish at the End of Casting

Mingtao Xuan, Min Chen, Kaizhu Zhang, and Xiaojie Hua

Abstract To increase the yield by decreasing the amount of residual molten steel in tundish, the vortex flow characteristics of the molten steel was investigated in a practical three-strand bloom tundish at the end of casting using physical and numerical simulation. The results showed that the vortex was strongly dependent to the asymmetric distribution of molten steel and the casting speed, so the vortex flow first occurred at strands 1 and 3, and the height of vortex formation was decreased by 25% while the casting speed was decreased from 0.65 to 0.48 m/min for the bloom with section size of 360 mm × 300 mm. Furthermore, the use of a square inhibiting baffle could disturb the upper fluid flow to decrease the height of vortex development by 23% at the casting speed of 0.48 m/min. Therefore, the installation of square inhibiting baffle is recommended, and the casting should be operated at lower casting speed.

Keywords Three-strand tundish · Vortex flow characteristics · Inhibiting baffle · Physical and numerical simulation

Introduction

Reducing inclusions and increasing alloy yield are an important issue to the alloy steel production. At the end of casting, vortexes can form above the submerged entry nozzle and entrap slag into the mold. The vortex slag entrainment can not only increase the inclusions in molten steel but also cause the oxidation of alloying elements. Moreover, some of the slag deposit in submerged entry nozzle internal surface and promote clogging. Although increasing the level height can inhibiting the vortex formation, but the alloy yield will decrease. Thus, the vortex flow characteristics in tundish at the end of casting are of crucial importance for the quality and cost of product.

M. Xuan · M. Chen (✉) · K. Zhang · X. Hua
School of Metallurgy, Northeastern University, Shenyang 110819, Liaoning, P. R. China
e-mail: chenm@smm.neu.edu.cn

Over recent years, free-surface vortex formation during liquid draining through a hole at the bottom of a vessel has been studied via physical and numerical simulation. Park and Sohn [1] investigated the air core in a circular tank by using experimental and computational methods. The critical height of vortex formation depended on the angular velocity of liquid. Li et al. [2, 3] used a mathematical model to analyze the mechanism and influencing factors of free-surface vortex formation during steel teeming process, and indicated that the initial tangential velocity and the position and diameter of nozzle had large effects on sink vortex formation. Although the phenomenon of free-surface vortex formation in the ladle is similar to that in the tundish, but the flow pattern in tundish is more complicated.

Solorio-Oiaz et al. and García-Hernández et al. [4, 5] studied a typical slab tundish by physical and numerical simulations, and indicated that even if the tundish was in normal operation, the unbalanced flow caused by the structure was still the source of the vortex formation. Meanwhile, the transient behavior of fluid flow was also an important reason for slag entrapment. Zhang et al. [6] studied the filling process in a practical tundish using VOF model and found that the unsteady flow pattern could cause slag entrapment and steel re-oxidation.

However, few works paid attention on the transient behavior of vortex flow at the end of casting. Ruan et al. [7] studied the free-surface formation and improved the unreasonable structure to prevent vortex flow in the slab tundish at the end of casting. Michalek et al. [8] developed a physical model to study the slag entrainment in a multi-strand billet tundish.

Despite researchers have studied the vortex formation and slag entrainment in the ladle and tundish by numerical and physical simulation, the vortex formation in bloom tundish was not well understood. The current work develops a mathematical model for investigating the transient behavior of vortex flow in a practical three-strand bloom tundish at the end of casting, and the control strategy was also discussed. The calculated results of this model were verified by water model experiments.

Model Descriptions

Physical Model

Based on the normal Froude similarity number [4], a 1:4 scaled physical model was established to study the characteristics and control strategy of vortex formation. Details of experiments could be found elsewhere. Table 1 gives the operating parameters and physical properties on the prototype and physical model.

Table 1 Operating parameters and physical properties in practical tundish and physical model

Parameter	Prototype	1/4 model
Casting speed (m³/h)	3110–4212	97–132
Mold width × thickness (mm²)	360 × 300	90 × 75
Height of initial liquid level (mm)	850	212.5
Liquid density (kg/m³)	7000	1000
Liquid viscosity (kg/(m·s))	0.0055	0.001
Gas density (kg/m³)	1.2	0.56
Gas viscosity (kg/(m·s))	1.82×10^{-5}	7.45×10^{-5}

Mathematical Model

Mathematical Formulations

The assumptions applied in the present multiphase flow of tundish can be found elsewhere. In this study, the VOF model coupled with RNG k-ε turbulence model was developed to capture the characteristics of vortex formation at the end of casting. Among them, the RNG k-ε turbulence model provided the flow pattern in the computational domain, and the VOF model was used to track the phase interface between air and molten steel. The general form of one mass equation, three momentum equations, and two standard k-ε turbulence equations could be expressed as Eq. (1).

$$\frac{\partial(\rho u_i \phi)}{\partial x_i} = \frac{\partial}{\partial x_i}\left(\Gamma_\phi \frac{\partial \phi}{\partial x_i}\right) + S_\phi \tag{1}$$

$$\alpha_{\text{air}} + \alpha_{\text{steel}} = 1 \tag{2}$$

where ρ is the fluid density, kg/m³; u_i is the speed in i direction, m/s; ϕ is the variables including velocities at three directions, temperature, enthalpy, turbulent kinetic energy, and dissipation rate, x_i is the direction, Γ_ϕ is the coefficient of diffusion, and S_ϕ is the source term. The flow parameters of the mixed fluid were calculated by the weighted average of the volume fractions of the phases. Furthermore, the Coriolis force was added into the momentum equation as a source term [7].

Computational Details

To reduce the computational cost, the computational domain was half of the tundish, as shown in Fig. 1a. Additionally, the square inhibiting baffle was used to delay the vortex formation, and its structure was shown in Fig. 1b.

At the wall in the domain, the zero-slip boundary condition was used. The outlet velocity was calculated by the flow rate. The top surface was set as a pressure inlet condition. To guarantee computational efficiency, the pressure implicit with splitting
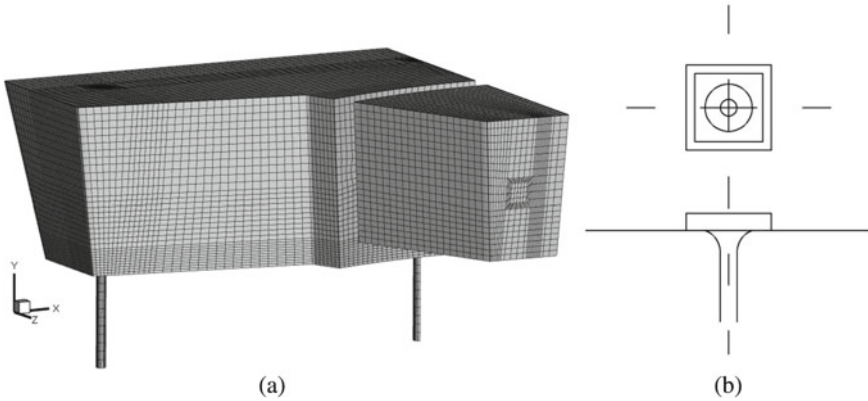
Fig. 1 Schematics of the simulation domain and square inhibiting baffle: **a** tundish model, **b** square inhibiting baffle

of operators (PISO) algorithm was chosen to solve the partial differential equation. A time step of 0.0005 s was used to ensure the stability of courant number in the transient process.

Results and Discussion

Vortex Formation Characteristics

To validate the developed mathematical model, a 1:4 scaled case was calculated to predict the free-surface vortex formation process and flow field in the water model of tundish at the casting speed of 0.48 m/min. Figure 2 shows the experimental and simulation results for the free-surface vortex formation at the strand 1. Compared with the figure in the physical model obtained by a camera, the phenomenon of free-surface vortex formation on the surface was captured well by numerical results. After the molten steel flows into the mold, the axial pressure gradient was increased in the
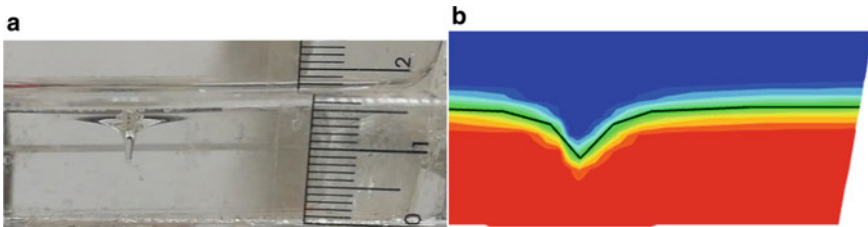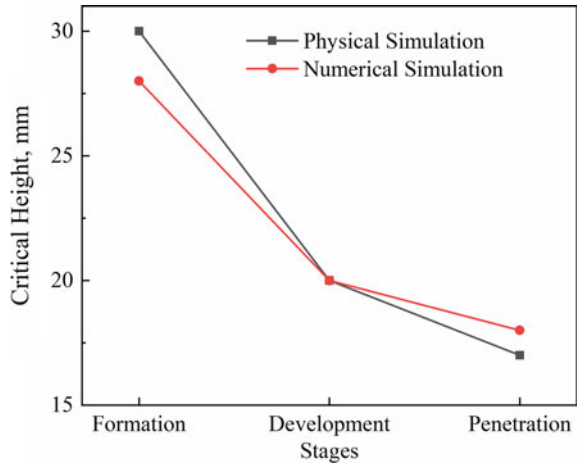

Fig. 2 Vortex formation obtained by **a** physical and **b** numerical simulation. (Color figure online)

Fig. 3 Volume fraction diagram at different stages of vortex. (Color figure online)

nozzle and forced the fluid into the nozzle. Therefore, the potential energy of molten steel was converted to kinetic energy, which was the source of vortex formation.

According to the experiments, the critical height of vortex formation at strand 2 was much smaller than that at strand 1, so this study only investigated the vortex formation at strand 1. Figure 3 shows the comparison of critical height between numerical simulation and physical modeling, in which three stages represented from the initial emergence to the final air-entrapment. All three stages were the formation, evolution, and penetration of vortex. In the formation stage, the vortex was formed in the tundish, and the free-surface was slightly deformed. With the process of casting, the angular momentum of molten steel near the nozzle gradually increased, which drove the upper liquid to rotate, causing the vortex to gradually develop. When the vortex extended to the nozzle, it was defined as the air-entrapment stage. In the same order as vortex development, the simulated critical heights was 28 mm, 20 mm, and 18 mm, respectively, which were in good agreement with the experimental results of 30, 20, and 17 mm.

Figure 4 shows the velocity distribution at different sections above the strand 1. At the free surface, which is 28 mm form the bottom of the tundish, the steel velocity was nearly 0.05 m/s, and the sink vortex was also formed. Several high velocity zones were found adjacent to the wall, and at the center of the tundish, and a clockwise vortex was formed by it. Figure 4b shows the velocity distribution 10 mm from the bottom. Compared with Fig. 4a, an increased flow velocity was detected, and the area of high velocity zones decreased. At the section 5 mm from the bottom, presented in Fig. 4c, the velocity distribution was centered on the nozzle, and the high velocity zones were narrowed further. In other words, the momentum of molten steel concentrated near the nozzle at the bottom and dissipated upward. This phenomenon indicated that amount of molten steel flowed form the walls to the nozzle and flowed from top to down, and this unbalance flow caused by asymmetric structures of tundish was the source of vortex formation.
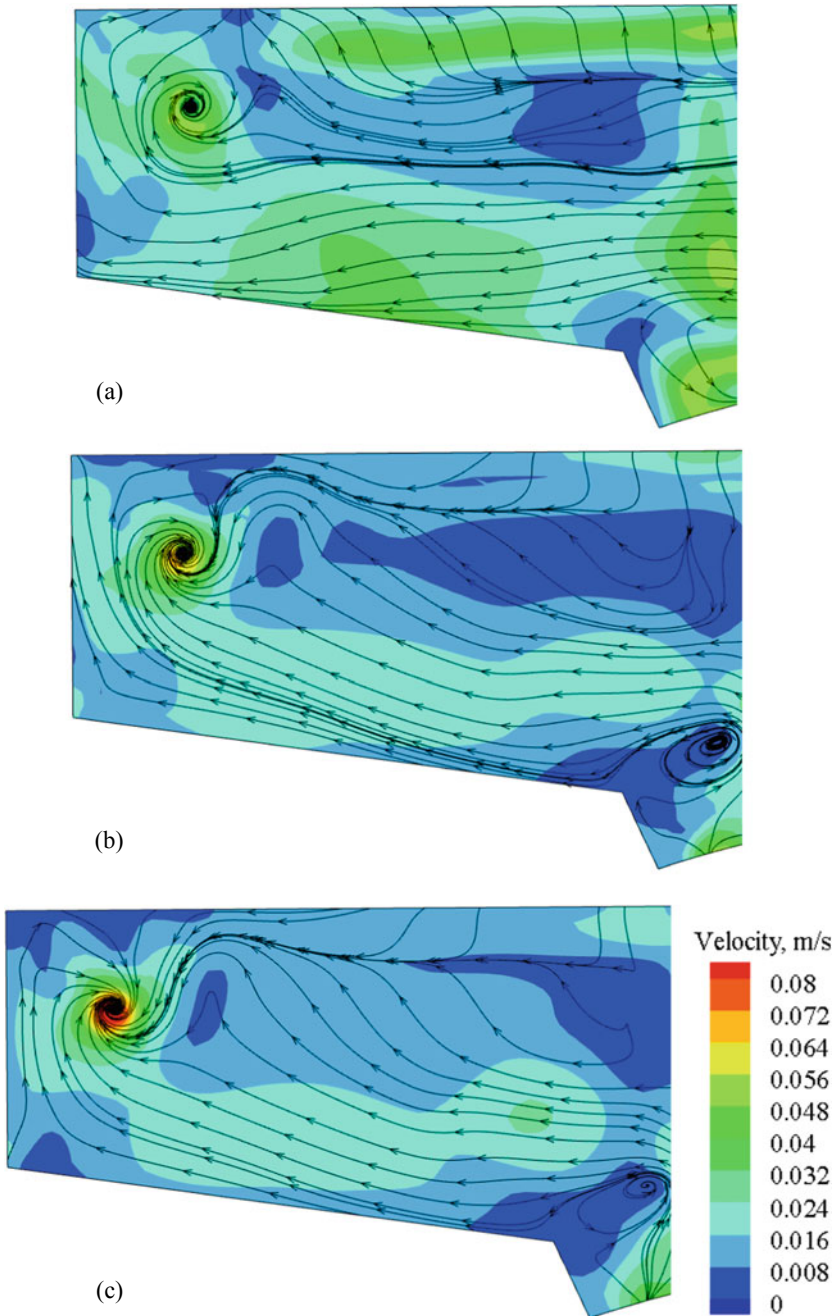
Fig. 4 Velocity distribution at different height from bottom: **a** free surface, **b** 10 mm, **c** 5 mm. (Color figure online)

Effect of Casting Speed

As mentioned previously in this study, the exit momentum at the end of continuous casting process had a significant effect on the flow pattern and promoted the vortex formation to the critical limits. Therefore, the effect of casting speed on vortex formation was studied in the practical tundish. For all cases, the simulation medium of molten steel and the similarity ratio of 1:1 were taken.

The velocity vector on the free surface 160 mm from the bottom of tundish are shown in Fig. 5. The simulation results correspond to two different casting speeds of 0.48 m/min and 0.65 m/min, respectively. At low casting speed (0.48 m/min), see Fig. 5a, the disturbance velocity was too low to form a distinct vortex, and the air-entrapment was not detect in this case. With the growing casting speed (0.65 m/min), as shown in Fig. 5b, a higher velocity developed on the interface, as well as a distinct vortex formed with air-entrapment. From the experimental results, when the casting speed increased to 0.65 m/min, the critical height of vortex formation was 40 mm, which was consistent with the numerical results.

Figure 6 shows the velocity distribution along the axis of the strand 1 nozzle corresponding to different casting speeds. For both the two cases, the velocity was very high in the nozzle, which meant the momentum dissipated less here. In the transition region, the velocity decreased rapidly with increasing the sectional area. Above the nozzle, the velocity continued to drop to near 0. Additionally, the results show that the velocity increased with casting speed; however, the velocity upon the nozzle was slightly increased, as shown in Fig. 5. This was because that most of the momentum was transferred to around rather than only above the nozzle. So the casting speed could be reduced, which was equivalent to reducing the momentum of molten steel in the tundish. The critical height of vortex formation could be decreased rapidly.
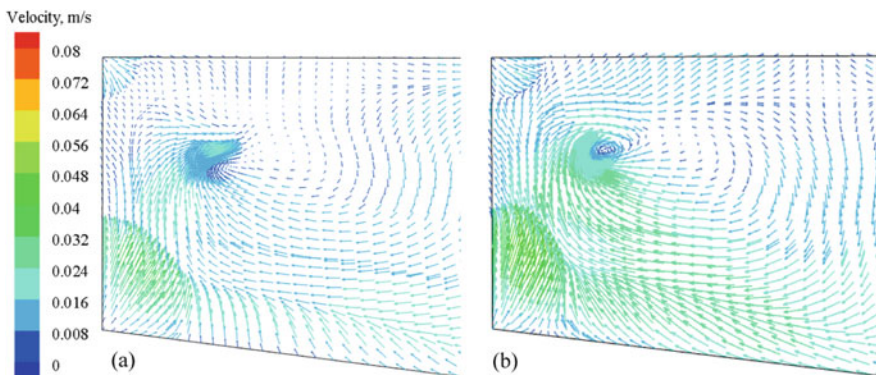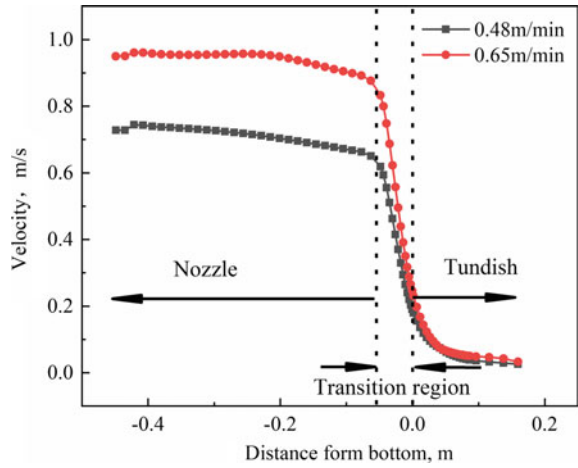

Fig. 5 Velocity vector diagram with liquid level of 160 mm at different casting speeds: **a** 0.48 m/min, **b** 0.65 m/min. (Color figure online)

Fig. 6 Velocity distribution along the axis of the nozzle. (Color figure online)

Control Strategy

According to the works ahead, the casting speed should be as small as possible to prevent the formation of vortex. However, due to the limitation of the heat energy and stable production, the casting speed should not be too low. Therefore, the casting speed of 0.48 m/min was taken in this section. The square inhibiting baffle was used to improve the flow pattern at the end of casting in the tundish and reduced the critical height of vortex formation. Figure 7 shows the simulation results of the square inhibiting baffle when the bath level is 90 mm.

Figure 7a shows that the free surface sank at this bath level which meant that the vortex was formed. For the original structure of tundish, the molten steel flowed directly into the nozzle. On the way to the nozzle, the molten steel flowed upward
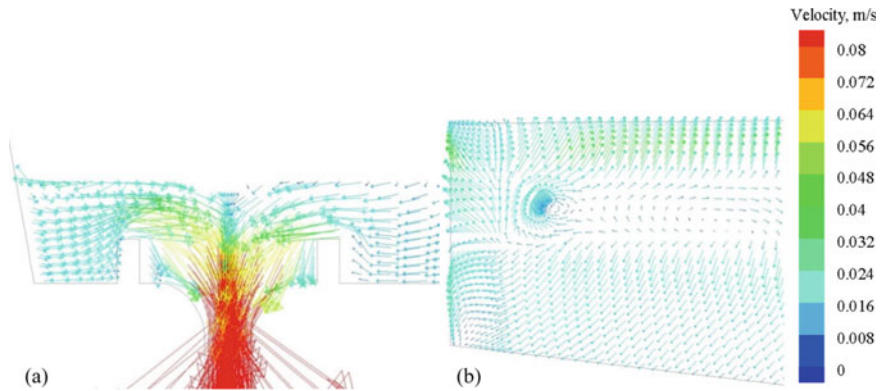

Fig. 7 Velocity vector diagram of vortex formation using square inhibiting baffle: **a** vertical section of nozzle center, **b** free surface. (Color figure online)

and passed through the square inhibiting baffle. This flow pattern increased the momentum loss and disturbed the upper fluid flow to the nozzle.

Figure 7b shows that the vortex was formed on the free surface. The square inhibiting baffle reduced the velocity and made it more even on the surface. Compared with the original tundish structure, the velocity difference on the surface was reduced, and the rotation speed upon the nozzle decreased. Therefore, the formation of vortex became more difficult, and the critical height reduced to 23 mm form experiments. Based on the experimental results and simulated results, the using of square inhibiting baffle could decreased the critical height of vortex formation significantly.

Conclusions

Based on the physical and numerical simulation, the transient vortex flow characteristics were investigated in a practical three-strand bloom tundish at the end of casting. Moreover, the control strategy was also discussed. The conclusions are as follows:

(1) The momentum of molten steel near the nozzle gradually spread around in the process of upward propagation and high velocity zones were formed near the wall. The asymmetric distribution of high velocity regions on the free surface was the source of vortex formation.
(2) The casting speed was a key parameter for the formation of vortex. As the casting speed increased, the critical height of vortex formation increased from 30 to 40 mm. So the casting speed should be as low as possible in this condition.
(3) The square inhibiting baffle could force the molten steel at the bottom flow upward to disturb the upper fluid flow to the nozzle. When the casting speed was 0.48 m/min, the using of square inhibiting baffle could decrease the critical height of vortex formation to 23 mm.

References

1. Park IS, Sohn CH (2011) Experimental and numerical study on air cores for cylindrical tank draining. Int Commun Heat Mass Transfer 38(8):1044–1049
2. Li HX, Wang Q, Lei H, Jiang JW, Guo ZC, He JC (2014) Mechanism analysis of free-surface vortex formation during steel teeming. ISIJ Int 54(7):1592–1600
3. Li HX, Wang Q, Lei H, Jiang JW, Guo ZC, He JC (2014) Analysis of factors affecting free surface vortex formation during steel teeming. ISIJ Int 56(1):94–102
4. Solorio-Oiaz G, Ramos-Banderas A, Barreto JJ, Morales RO (2007) Fluid dynamics of vortex formation in tundish operations: physical modelling. Steel Res Int 78(3):248–253

5. García-Hernández S, Solorio-Diaz G, Ramos-Banderas JA, Barreto JJ, Morales RD (2009) Fluid dynamics of vortex formation in tundish operations: mathematical modelling. Steel Res Int 80(4):256–263
6. Zhang H, Luo RH, Fang Q, Ni HW, Song X (2018) Numerical simulation of transient multiphase flow in a five-strand bloom tundish during ladle change. Metals. https://doi.org/10.3390/met802 0146
7. Ruan YW, Yao Y, Shen SY, Wang B, Zhang JY, Huang JK (2020) Physical and mathematical simulation of surface-free vortex formation and vortex prevention design during the end of casting in tundish. Steel Res Int. https://doi.org/10.1002/srin.201900616
8. Michalek K, Gryc K, Socha L, Tkadleckova M, Saternus M, Pieprzyca J, Merder T, Pindor L (2016) Study of tundish slag entrapment using physical modelling. Arch Metall Mater 61(1):257–260